

## Article

# New Composites Derived from the Natural Fiber Polymers of Discarded Date Palm Surface and Pineapple Leaf Fibers for Thermal Insulation and Sound Absorption

Mohamed Ali <sup>\*</sup>, Zeyad Al-Suhaibani , Redhwan Almuzaiqer, Ali Albahbooh <sup>†</sup>, Khaled Al-Salem  and Abdullah Nuhait

Mechanical Engineering Department, College of Engineering, King Saud University, P.O. Box 800, Riyadh 11421, Saudi Arabia; 438106677@student.ksu.edu.sa (A.A.); kalsalem@ksu.edu.sa (K.A.-S.)

<sup>\*</sup> Correspondence: mali@ksu.edu.sa

<sup>†</sup> MS graduate student.

**Abstract:** New composites made of natural fiber polymers such as wasted date palm surface fiber (DPSF) and pineapple leaf fibers (PALFs) are developed in an attempt to lower the environmental impact worldwide and, at the same time, produce eco-friendly insulation materials. Composite samples of different compositions are obtained using wood adhesive as a binder. Seven samples are prepared: two for the loose natural polymers of PALF and DPSF, two for the composites bound by single materials of PALF and DPSF using wood adhesive as a binder, and three composites of both materials and the binder with different compositions. Sound absorption coefficients (SACs) are obtained for bound and hybrid composite samples for a wide range of frequencies. Flexural moment tests are determined for these composites. A thermogravimetric analysis test (TGA) and the moisture content are obtained for the natural polymers and composites. The results show that the average range of thermal conductivity coefficient is 0.042–0.06 W/(m K), 0.052–0.075 W/(m K), and 0.054–0.07 W/(m K) for the loose fiber polymers, bound composites, and hybrid composites, respectively. The bound composites of DPSF have a very good sound absorption coefficient (>0.5) for almost all frequencies greater than 300 Hz, followed by the hybrid composite ones for frequencies greater than 1000 Hz (SAC > 0.5). The loose fiber polymers of PALF are thermally stable up to 218 °C. Most bound and hybrid composites have a good flexure modulus (6.47–64.16 MPa) and flexure stress (0.43–1.67 Mpa). The loose fiber polymers and bound and hybrid composites have a low moisture content below 4%. These characteristics of the newly developed sustainable and biodegradable fiber polymers and their composites are considered promising thermal insulation and sound absorption materials in replacing synthetic and petrochemical insulation materials in buildings and other engineering applications.



**Citation:** Ali, M.; Al-Suhaibani, Z.; Almuzaiqer, R.; Albahbooh, A.; Al-Salem, K.; Nuhait, A. New Composites Derived from the Natural Fiber Polymers of Discarded Date Palm Surface and Pineapple Leaf Fibers for Thermal Insulation and Sound Absorption. *Polymers* **2024**, *16*, 1002. <https://doi.org/10.3390/polym16071002>

Academic Editor: Zina Vuluga

Received: 13 March 2024

Revised: 2 April 2024

Accepted: 4 April 2024

Published: 6 April 2024

**Keywords:** date palm surface fibers; pineapple leaf fibers; thermal conductivity coefficient; sound absorption coefficient; agro-waste utilization



**Copyright:** © 2024 by the authors. Licensee MDPI, Basel, Switzerland. This article is an open access article distributed under the terms and conditions of the Creative Commons Attribution (CC BY) license (<https://creativecommons.org/licenses/by/4.0/>).

## 1. Introduction

Agro-waste materials are available in huge amounts and are biodegradable, sustainable, eco-friendly, and natural. These wasted materials have to be recycled efficiently; otherwise, they create a burden on the environment. The Organization of Agriculture and Food [1] has reported that Saudi Arabia is one of the largest countries in terms of date production, producing 1.2 million tons/year. The huge amount of waste that can be produced from the date palm trees has many useful applications, such as pulp paper production and as composite materials using fibers [2–4]. Furthermore, 20 kg of leaves can be produced from each date palm tree per year as waste. Moreover, atmospheric pollution could occur if such waste is burned in the air, as usually happens as a common practice in some areas of the world [5]. Therefore, good utilization of such wastes will have a good

environmental impact in addition to economic benefits. Eleven million tons of agricultural waste per year can be produced in Saudi Arabia, and most of them belong to date palm trees. Those wastes have valuable benefits from an economic point of view [6,7]. Date palm spikelet and date palm fiber have been used with the bricks to improve their thermal insulation characteristics by Belatrache et al. [8]. Their results showed that the thermal conductivity coefficient of the new bricks was  $0.106 \text{ W}/(\text{m K})$  when 1.36% of date palm fiber was used. Raza et al. [9] have developed a new composite made of date palm surface fiber and polystyrene as a new insulation material for buildings. Their new composite with 20% date palm surface fiber had a low thermal conductivity coefficient of  $0.053 \text{ W}/(\text{m K})$ . Four samples of date palm surface fibers were developed at different densities for thermal insulation by Raza et al. [10] using polyvinyl alcohol as a binder. Their results showed an average thermal conductivity coefficient of  $0.038\text{--}0.051 \text{ W}/(\text{m K})$ . Ali and Abdelkareem [11] have reported new thermal insulation materials extracted from date palm surface fibers. The thermal conductivity coefficient range of their produced sample boards was between  $0.0475$  and  $0.0697 \text{ W}/(\text{m K})$  using cornstarch resin as a binder. Ali et al. [12] have developed natural insulation materials as a composite between date palm tree leaves and wheat straw fibers. The thermal conductivity of their boards was in the range of  $0.045\text{--}0.065 \text{ W}/(\text{m K})$  at temperatures of  $10\text{--}60 \text{ }^\circ\text{C}$ , respectively, using wood adhesive as a binder. Alabdulkarem et al. [13] have developed new experimental thermal insulation materials made as a hybrid between Apple of Sodom fibers and date palm surface fibers with different compositions using wood adhesive, corn starch, and white cement as binders. Their boards had average thermal conductivity coefficients in the range  $0.04234\text{--}0.05291 \text{ W}/(\text{m K})$ , and the absorption coefficient of the boards was also determined to be greater than 0.5 at high frequency.

On the other hand, the solid waste, which is a by-product of pineapple industries, is in the range of 40–50% from the peelings, crown, and core (Buckle, [14]). Adhika et al. [15] have reported that the sound absorption coefficient of pineapple fiber with an epoxy composite is greater than 0.5 at high frequencies, and it was affected by the density and applied pressure of the sample. Pineapple leaves were reported as good thermal insulation materials by Tangjuank [16]. He used natural rubber latex as a binder for boards with different densities, and the measured thermal conductivity was in the range of  $0.035 \text{ W}/\text{m K}$  to  $0.043 \text{ W}/\text{m K}$ . The same binder is used by Kumfu and Jintakosol [17] in producing a thermal insulation board with a density of  $338 \text{ kg}/\text{m}^3$  from pineapple leaves with a thermal conductivity coefficient of  $0.057 \text{ W}/(\text{m K})$ . Hybrid of pineapple fibers and polyester using a needle-punching technique was used in developing nonwovens by Thilagavathi et al. [18]. Their product had better thermal insulation and sound-absorbing characteristics compared to pure pineapple fibers. Aerogel composites were made of cotton waste and pineapple leaf by Do et al. [19]. That aerogel was tested as a thermal insulation, and its thermal conductivity coefficient was found in the range of  $0.039\text{--}0.043 \text{ W}/(\text{m K})$ . Pineapple leaf fibers with paper waste composites were examined for their sound absorption as an alternative to synthetic fiber by Sari et al. [20]. Their results showed that the sound absorption coefficient increased as the pineapple leaf fibers increased in the composites at the expense of the impact strength. Suphamitmongkol et al. [21] have used pineapple leaf fiber (PALF) as a potential source of sound absorption and thermal insulation materials. They showed that the thermal characteristics of the composites made of PALF were better than those with PET and asbestos but comparable to the composites made of glass fiber. On the other hand, they found that the acoustic properties of PALF are better than those of glass fiber but lower than polyester fiber. Recently, Ali et al. [22] have experimentally studied the effect of using natural polymers of PALF, sunflower seeds, and watermelon seeds and their hybrid composites as new thermal insulation and sound absorption materials. Their results showed that the average thermal conductivity for the composite of PALF and the sunflower seeds was  $0.05921 \text{ W}/(\text{m K})$  and  $0.06577 \text{ W}/(\text{m K})$  for the composite of PALF and the watermelon seeds. The sound absorption coefficient was found above 0.5 for most of the bound and hybrid composites. New bio-degradable composite foams made of pineapple stem starch and pineapple leaves were reported by Namphonsane et al. [23]. Their results

indicated that the flexural strengths of the composite foams ranged from 1.5 to 4.5 MPa. Furthermore, the sound absorption coefficient of natural fibers such as corn, sugar cane, coir, and dry grass was measured for different thickness samples by Fouladi et al. [24] and found to be good alternatives for common building acoustic boards. Noise reduction and sound absorption coefficients were reported for hemp, kenaf, coconut, cork, sheep wool, cardboard, and cane by Berardi and Iannace [25]. They have shown that these coefficients were thickness, density, and porosity-dependent, and they have been recommended for use in buildings.

Most of the literature mentioned above focused on using natural fiber polymers of DPSF and PALF only; however, bound or hybrid composites were not considered. Therefore, this study presents new novel bound and hybrid composite boards made of date palm surface fibers and pineapple leaf fibers as thermal insulation and sound-absorbing materials. Different densities and composition boards are made, and their thermal conductivity and sound absorption coefficients are found to be promising to use as applications in buildings and can be considered as good biodegrading ecofriendly materials in replacing the synthetic and petrochemical ones.

## 2. Materials and Methods

### 2.1. Collecting the Discarded Materials

At a specified time of the year, the agricultural authority trims a huge amount of date palm trees, wherein they get rid of the residual of such trees, such as date palm surface fibers and leaves. Therefore, those wasted surface fibers are gathered and collected from the authorities before they get rid of them in landfills and create an environmental problem. The pineapple leaves are collected in the same way from the nearby farms in the areas that grow pineapple trees. Another source of pineapple leaves is usually the local juice stores, which get rid of a large amount of the pineapple fruit's crown, which contains many leaves that are disposed of as waste daily. Figure 1a,b show both the date palm surface fibers and pineapple leaves, respectively. The collected date palm surface fibers are cut to approximately 15 cm in length. The collected pineapple leaves and date palm surface fibers are washed with water to get rid of any dust or other impurities. After that, they are dried either in a covered solar cooker (already exists to save energy) (Figure 2a,b) for sunny days, where the maximum inside temperature reaches 90 °C, or in an electric convection oven at 100 °C, as shown in Figure 2c. The dried natural pineapple leaves are ground in a blender to pieces of an average length of 0.5–3 cm. It should be noted that both natural fiber polymers of DPSF and PALF are used after drying for thermal conductivity measurement with no chemicals or any other treatment. The bound and hybrid composites are moved to the drier after compression in the mold.



**Figure 1.** Loose fibers: (a) date palm surface fibers (DPSFs) and (b) pineapple leaf fibers.

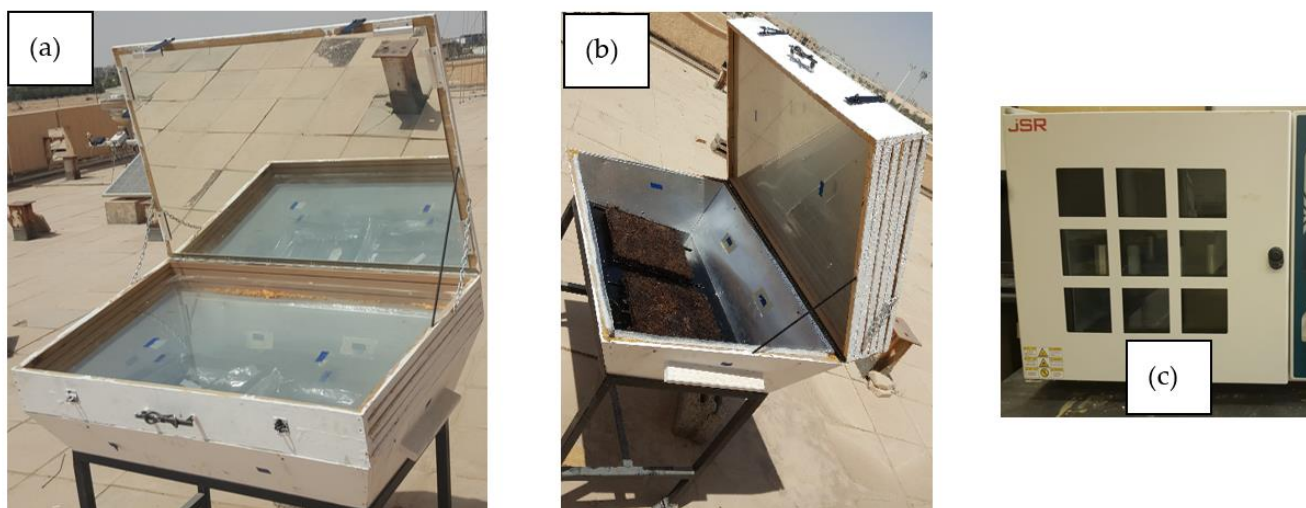


**Figure 2.** Solar cooker oven ((a) closed and (b) open) and (c) electric convection oven.

## 2.2. Preparing the Samples for Testing

The dried sample boards are prepared in three groups: loose fiber polymers and bound and hybrid composite groups.

### 2.2.1. Loose Fiber Polymer Group Samples

These groups include the PALF and the DPSF after collecting, washing, and drying them, as described earlier in Section 2.1. The loose fiber polymer samples are enclosed in a wooden mold with inside dimensions of  $26.5 \times 26.5 \times d$  cm<sup>3</sup>, where  $d$  is the thickness, as shown in Figure 3a,b, to be fitted inside the heat flow meter for thermal conductivity measurement.



**Figure 3.** Loose fibers in the wooden mold: (a) PALF and (b) DPSF.

### 2.2.2. Bound Composite Group Boards

The wood adhesive binder (polyvinyl acetate resin) is used to bind the loose polymer samples. Full specifications, ingredients, and physical and chemical properties of the binder can be found in [26]. A solution of water and wood adhesive is prepared (350 g of the binder and 800 g of water), and the loose leaves or fibers are immersed in it to be sure that each leaf or fiber is in contact with the binder solution. Then, the wetted samples are moved to a stainless mold (Figure 4a), followed by a cold presser to press the sample to a specified size. The load used in pressing the composites is about 173 N, which makes the pressure about 1922 Pa. It should be mentioned that during pressing the composite, the excess solution is discharged; therefore, the actual amount of used adhesive is estimated after

the drying process since the mass of the dried fiber is known beforehand. The estimated polymerized mass of the adhesive is introduced in Table 1 with its percentage ratio to the total mass of the composite. After that, the samples are moved either to the solar cooker oven or the electric convection oven for drying, as described in Section 2.1. The dried bound samples are then taken off the mold (Figure 4e) and moved to the heat flow meter for thermal conductivity measurement. Figure 4 summarizes these processes. It should be noted that adding binders to the loose natural polymer fibers increases their thermal conductivity; therefore, one should use the binder, which has a low effect on the thermal conductivity. In our previous study [13], we compared three different binders, namely cornstarch, wood adhesive, and white cement, and the result confirmed that wood adhesive has a lower effect on the thermal conductivity coefficient.

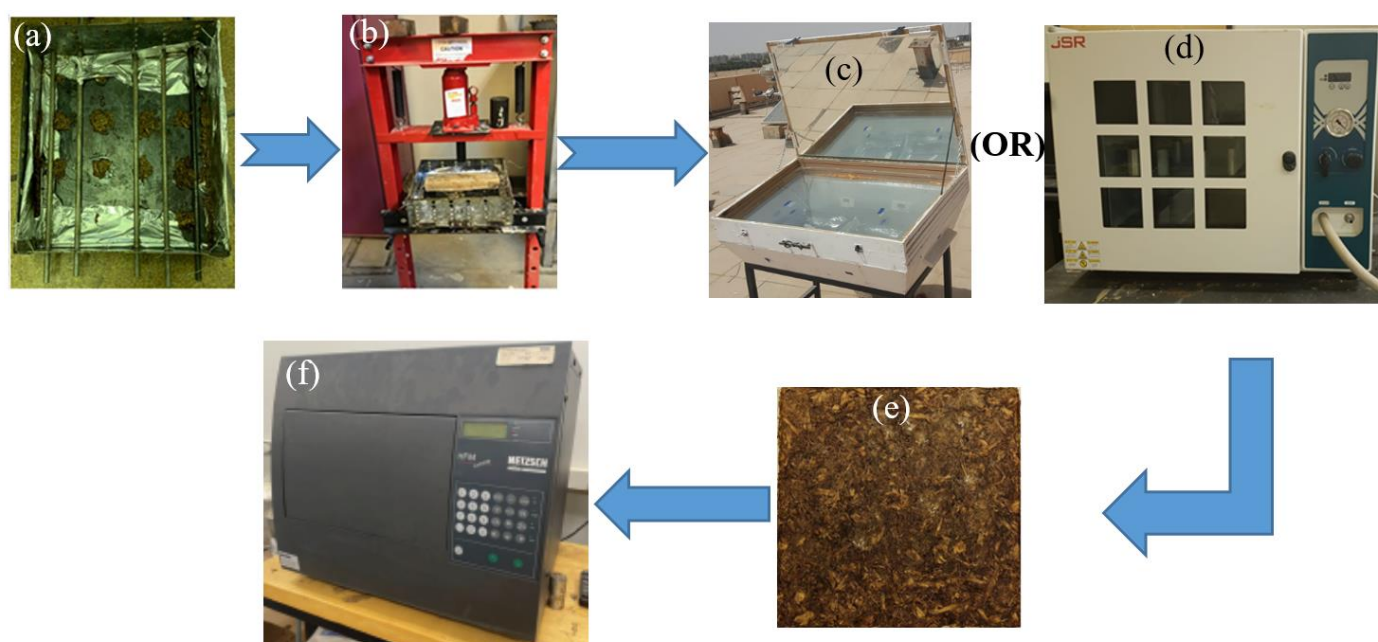


**Figure 4.** Process of preparing the bound or hybrid polymer samples: (a) stainless steel mold holding the sample, (b) presser, (c) drying solar oven, (d) drying electric oven, (e) the removed dried sample, (f) the heat flow meter for thermal conductivity measurement.

**Table 1.** Physical properties and dimensions of the developed polymer samples.

Material	Sample Number						
	Lo (# 1)	Bo (# 2)	Lo (# 3)	Bo (# 4)	Hy (#5)	Hy (#6)	Hy (# 7)
DPSF %	0.0	0.0	100	75.9	46.0	33.0	18.0
Mass of DPSF (g)	0.0	0.0	500	500.2	272.3	150.15	107.6
PALF %	100	87	0.0	0.0	15.0	33.0	53.0
Mass of PALF (g)	106	321.9	0.0	0.0	88.8	150.15	317.0
The ratio of the polymerized binder to the total mass %	0.0	13	0.0	24.1	39.0	34.0	29.0
Mass of the binder (g)	0.0	48.1	0.0	158.8	230.9	154.7	173.4
Thickness, (mm)	21.0	13.0	46.0	44.0	30.0	30.0	24.0
Figure #	3a	5a	3b	5b	5c	5d	5e
Density of dried specimen (kg/m <sup>3</sup> )	76.5	329	121	166	212	169	277
Total dried mass (g)	106	370	500	659	592	455	598

### 2.2.3. Hybrid Composite Group Boards

Hybrid composite boards are those samples made of PALF and DPSF by different compositions using the same resin and method described in Section 2.2.2. Figure 5 shows the laboratory-prepared bound and hybrid composite boards. Table 1 shows the complete specification of all developed samples. It should be noted that the bulk density that appears in Table 1 was calculated by measuring the volume of each dried composite (Figure 5) and its mass; then, the density is obtained as the ratio of the mass over the volume. The same procedure was used in calculating the density of the loose polymers, as shown in Figure 3.

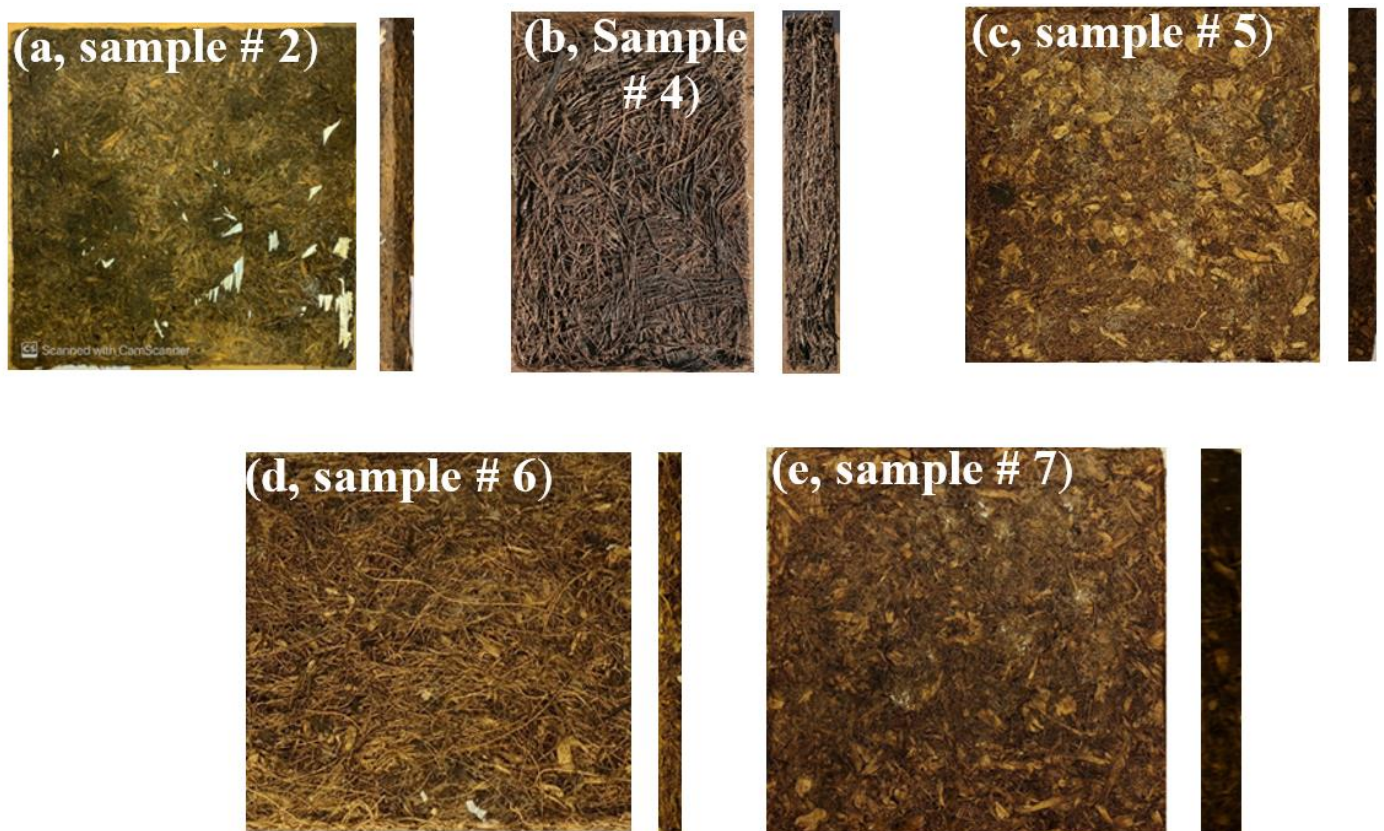


**Figure 5.** Bound and hybrid composite boards of PALF and DPSF: (a) bound composite PALF (# 2), (b) bound composite DPSF (# 4), (c) hybrid composite of PALF + DPSF (# 5), (d) hybrid composite of PALF + DPSF (6), and (e) hybrid composite of PALF + DPSF (# 7).

### 3. Mechanical Test for Bound and Hybrid Composite Samples

The three-point flexural test is obtained for both bound and hybrid composites. Figure 6 shows the specimen used for that test and its dimensions.

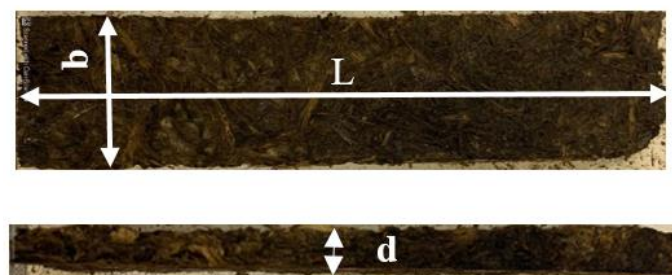


**Figure 6.** The specimen dimensions used in the three-point flexural test.

The universal testing machine (INSTRON 5984, UTM) with a cross-head of 2 mm/min, which is attached with three points of flexion, is used to perform the flexural test. The flexural stress  $\sigma_f$  and flexural strain  $\epsilon_f$  were recorded for each specimen at all applied loads following Equations (1) and (2), respectively, and the flexural modulus  $E_f$  from Equation (3).

$$\sigma_f = \frac{3F(L1)}{2bd^2} \quad (1)$$

$$\epsilon_f = \frac{6Dd}{(L1)^2} \quad (2)$$

$$E_f = \frac{(L1)^3 m}{4bd^3} \quad (3)$$

The software of the machine provides the deflection  $D$  at each load, where  $F$ ,  $L$ ,  $b$ ,  $d$ , and  $m$  are the load (force) at the fracture point, length of the specimen (20 cm), width, thickness, and the gradient (slope) of the initial straight-line portion of the load-deflection curve of the specimen, respectively. Table 2 shows the dimensions of the used specimens. This test follows the ASTM D790-03 standard [27].

**Table 2.** Dimensions of the flexural specimens.

Specimen No.	Thickness $d$ (mm)	Width $b$ (mm)	Span ( $L1$ ) (mm)
2	13.5	49.5	150
4	43	59.50	130
5	23	55.0	150
6	30	51.0	150
7	23	55.0	150

#### 4. Scanning Electron Microscopy (SEM) Analysis

The surface morphology of the loose, bound, and hybrid composites is determined at different magnifications by using the SEM of type (FE-SEM) (JEOL company, model number JSM7600F, Peabody, MA 01960, USA). A mandatory step before performing the test is to oven-dry the sample first and then coat it with platinum to avoid any electrostatic charging, which may happen during the test. It should be noted that the bound and hybrid composites used for the SEM scanning are obtained from the samples before the mechanical testing, where the objective is focused on the fiber shape and size of the composite and the polymerized binder.

#### 5. Thermal Conductivity Coefficient Measurement Test

The heat flow meter (HFM) shown in Figure 4f is used for this test. This HFM is of the bench type (HFM 436 Lambda) manufactured by the German company NETZSCH (NETZSCH-Gerätebau GmbH). This HFM is in accordance with the standards ASTM C518 [28], ISO 8301 [29], JIS A1412 [30], and DIN EN 12667 [31]. The tested samples must have dimensions of  $30 \times 30 \times d$  cm<sup>3</sup>, where  $d$  is a variable thickness up to 10 cm. The thermal conductivity coefficient for any sample can be determined at any temperature between 20 and 80 °C. Its theory depends on the hot and cold plates, where the heat flows between them at a mean temperature of 20 °C. The thermal conductivity coefficient and temperature accuracy are  $\pm 1\%$  to  $3\%$  W/(m K) and  $\pm 0.01$  °C, respectively (manufacturer's catalog). This HFM is used to determine the thermal conductivity coefficients for either the loose polymer samples shown in Figure 3 or the bound and hybrid composite ones shown in Figure 5. The thermal conductivity coefficient is measured at a wide range of temperatures since the environment temperature in hot weather regions could reach about 45 °C to 50 °C. This wide range of temperatures can also provide the thermal conductivity coefficient dependent on temperature for the new composite materials.

## 6. Sound Absorption Coefficient Test

Sound absorption tests are determined for both bound and hybrid sample numbers 2–7. Two impedance tube sizes are used for a wide range of frequencies: one with a 100 mm diameter for a frequency range of 63–1600 Hz by interchanging the position of the two used microphones and the other with a 30 mm diameter tube for a frequency range of 800–6300 Hz. The software VA-Lab IMP (Ver: V1. 03) was designed by BSWA (BSWA Technology Co., Ltd., Beijing, China), which conforms to ISO 10534-1 [32] and ISO 10534-2 [33] standards. More details and specifications can be found in [34].

## 7. Thermal Stability and Decomposition Test

Thermal stability and decomposition analysis are determined by the thermogravimetric analysis (TGA) and its differential thermogravimetric analyses (DTGAs) for the loose natural polymers of pineapple leaf fibers (PALFs), date palm surface fiber (DPSF), the composite of the bound fibers (# 2 and # 4), and the hybrid composite number 5. Testing Analytical Instrument (TA) TGA Q50 V20.10 Build 36 setup is used. The manufacturer is the Waters Corporation (New Castle, DE 19720, USA). A small amount of each kind of polymer or composite is contained in a platinum pan during the heating up to 600 °C or more. The heating starts at 26 °C at a heating rate of 10 °C/min, and the mass flow rate of the nitrogen gas is 100 mL/min.

## 8. Moisture Content Test

The moisture content test is carried out for the raw loose material of PALF, DPSF, bound composites, and hybrid composites following ASTM D2974-07A [35] standard. Some of each sample is dried in a convection oven (Figure 4d) for one full day, and their mass is denoted as  $m_2$ . The mass is left in the laboratory at a temperature and relative humidity of 21.6 °C and 51.7%, respectively, where their mass is scaled and recorded every five minutes and noted  $m_1$ . The difference between  $m_1$  and  $m_2$  presents the moisture content absorbed by the material. This percentage of the absorbed moisture content can be calculated from

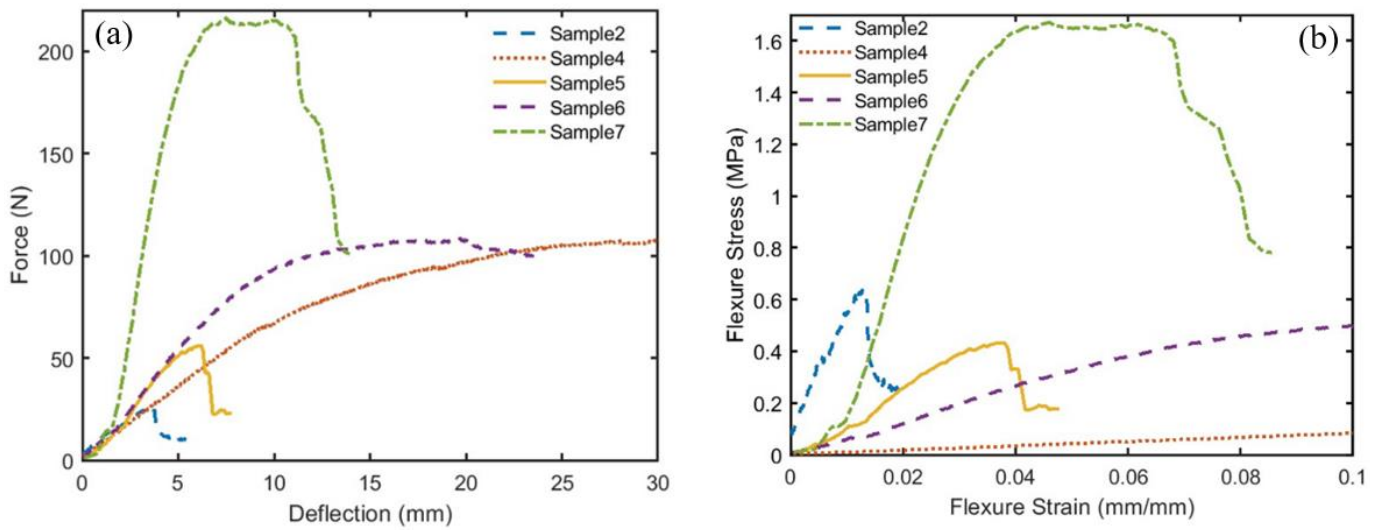
$$\% \text{ of moisture content} = \frac{m_1 - m_2}{m_2} \times 100 \quad (4)$$

## 9. Results and Discussion

Figure 7a,b show the force-deflection profiles and the flexure stress–strain curves, respectively, for the bound composite numbers 2 and 4 and the hybrid ones, numbers 5, 6, and 7. The flexural sample's dimensions are listed in Table 2, and the calculated mechanical properties, such as flexural stress  $\sigma_f$ , flexural strain  $\epsilon_f$ , and flexural modulus  $E_f$ , are shown in Table 3. These parameters are evaluated following Equations (1)–(3) above. Table 3 presents the maximum  $\sigma_f$  before the deviation from linearity [36] (Figure 7b), where the flexural strain  $\epsilon_f$  is obtained. It should be noted that the slope ( $m$ ) is calculated from the linear straight line of the profiles in Figure 7a.

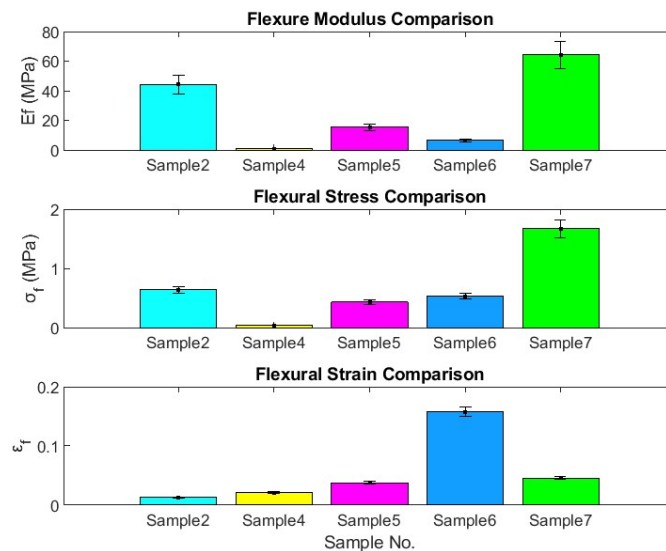
**Table 3.** Mechanical properties of the three-point flexural tests.

Specimen No.	Slop, $m$ (N/mm)	Flexure Modulus (MPa), $E_f$	Density, $\text{kg/m}^3$	Flexural Stress (MPa), $\sigma_f$	Flexural Strain at Flexural Strength, $\epsilon_f$
2	6.4	44.2 ± 5.9	329	0.64 ± 0.057	0.01 ± 0.001
4	6.5	0.8 ± 0.1	166	0.04 ± 0.003	0.02 ± 0.001
5	12.3	15.4 ± 2.1	212	0.43 ± 0.039	0.04 ± 0.002
6	10.6	6.5 ± 0.9	169	0.53 ± 0.047	0.16 ± 0.007
7	50.9	64.2 ± 8.6	277	1.67 ± 0.149	0.05 ± 0.002



**Figure 7.** Three-point flexural test results for the bound and hybrid samples: (a) force-deflection profiles and (b) flexure stress–strain curves.

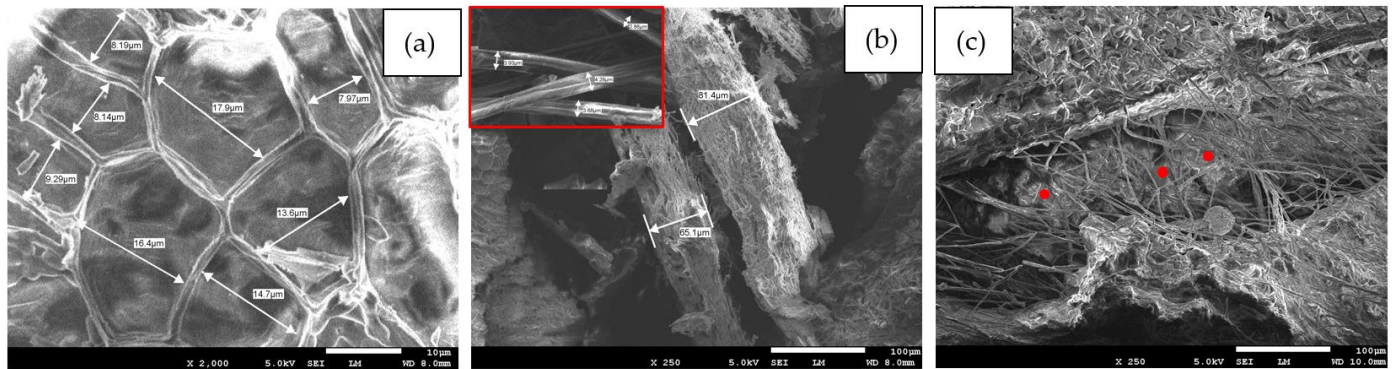
It is worth mentioning that an enhancement is observed in both  $E_f$  and  $\sigma_f$  as the density of the specimen increases, which agrees very well with the results obtained by [37,38]. Therefore, specimen number 7 is the best among the hybrid composites, while number 2 is the best among the bound composite specimens. Figure 8 compares the mechanical properties of the hybrid and bound samples in terms of bar charts with error bars. It should be noted that the compactness degree plays a very important role in enhancing the flexural modulus  $E_f$ , flexural stress  $\sigma_f$ , and  $\epsilon_f$ . This compactness depends on the polymerized binder ratio and the density of the specimen. The error in measuring the length, slope, deflection, and load is  $\pm 1.0$  mm,  $\pm 0.7$  N/mm,  $\pm 0.001$  mm, and  $\pm 1.0$  N, respectively. A computer program is written to calculate the absolute uncertainty and its percentage following the procedure described by McClintock [39] and Moffat [40]. The maximum uncertainties of flexural modulus ( $E_f$ ), flexural stress ( $\sigma_f$ ), and flexural strain ( $\epsilon_f$ ) are 13.4%, 8.9%, and 4.6%, respectively.



**Figure 8.** Comparison of the mechanical properties of the bound and hybrid composite samples.

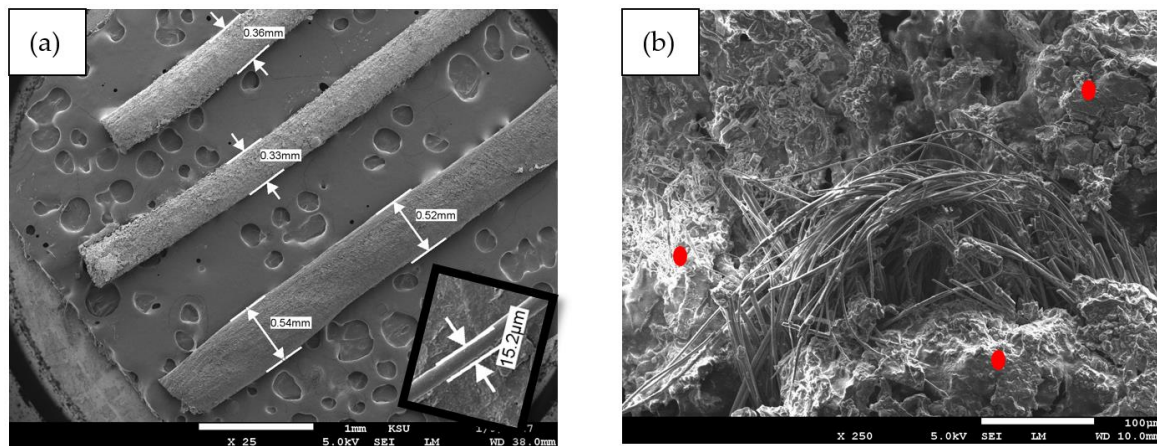
Figure 9a,b show a surface morphology comparison of the loose (Lo # 1) and bound composite (Bo # 2) of PAlF. Figure 9a shows the texture shape of the loose leaf at 2000 magnification, while Figure 9b shows that after being ground in a blender, where the thickness

of the leaves is in the range of 2.86–81.4  $\mu\text{m}$ . Figure 9c shows the composite after mixing and compressing with the binder. Red spots show some of the polymerized binders. It is also noticed that there are a lot of cavities between the skinny fibers, which in turn enhances the thermal conductivity and the sound absorption coefficient, as shown in the next sections.



**Figure 9.** PALF: (a) texture of the loose fiber polymers (Lo # 1) at 2000 magnification, (b) thickness of the ground leaves, and (c) composite (Bo # 2); red spots show the polymerized binder.

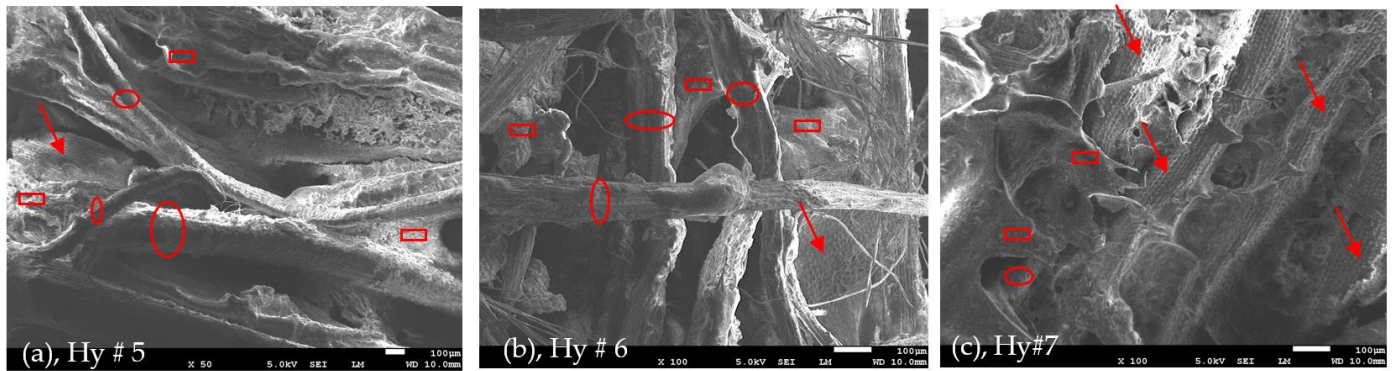
Figure 10a,b show the same configuration but for the DPSF, where Figure 10a shows the size of the loose rough fiber between 15.2  $\mu\text{m}$  and up to 0.54 mm outside diameter. Red spots show the polymerized binders hugging the fibers, leaving some void cavities. It should be noted that the lower corner of Figure 10a shows the small fiber size with larger magnification taken from another photo and montaged here to conserve the number of figures.



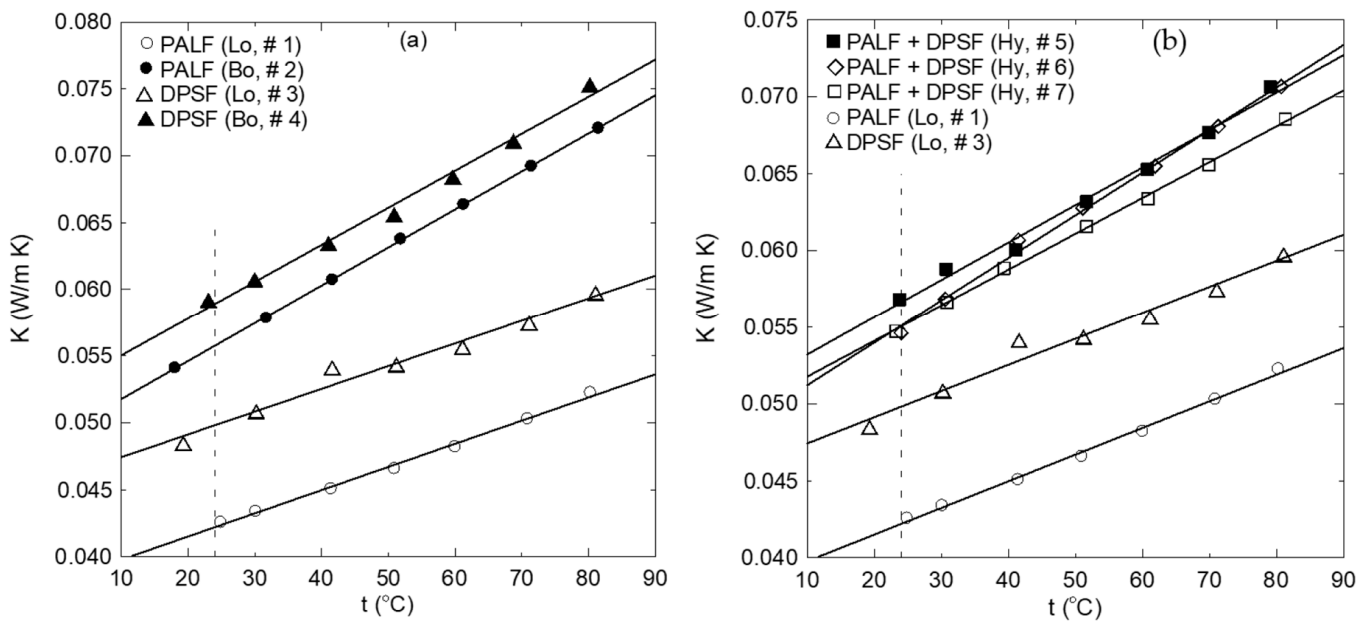
**Figure 10.** DPSF surface morphology at 250 magnification: (a) loose fiber polymers (Lo # 3) at 25 magnification and (b) bound composite (Bo # 4) at 250 magnification.

Figure 11a–c show similar surface morphology of the hybrid composite samples 5, 6, and 7, respectively. It should be mentioned that the red arrows, ellipses, and rectangles denoted some of the textures of the PALF, DPSF, and binder, respectively. Figure 12a compares the thermal conductivity coefficient ( $K$ ) of both loose date palm surface fiber (DPSF, Lo, # 3) and pineapple leaf fibers (PALFs, Lo, # 1) with their bound samples (Bo, # 2 and # 4). Adding binders increases the thermal conductivity coefficient since most of the little porous void spaces in the loose samples get filled with the polymerized binder [22,41,42]. Solid lines present the best curve-fitting through the data. The vertical dashed line at an ambient temperature of 24  $^{\circ}\text{C}$  shows that  $K$  for all samples is below 0.06  $\text{W}/(\text{m K})$ , which indeed promotes these discarded waste polymer and composite materials as good thermal insulation for buildings. Figure 12b compares the loose samples of both fibers to that of

hybrid composite numbers 5, 6, and 7 at different compositions, as shown in Table 1. It should be noted that K depends on the amount of polymerized binder used since more binders mean more void porous pores will be filled, which tends to increase K.



**Figure 11.** Hybrid composite surface morphology of DPSF and PALF and the binder. (a) Hy # 5 composite at 50 magnification, (b) Hy # 6 composite at 100 magnification, and (c) Hy # 7 at 100 magnification, see text for details.



**Figure 12.** Thermal conductivity coefficient profiles for (a) loose and bound samples of DPSF and PALF and (b) loose and hybrid samples of DPSF and PALF.

Furthermore, the degree of compactness also tends to reduce those pores, which also increases K. In addition, for the same material, increasing the density tends to increase K for the same reason. Moreover, the thermal conductivity depends on the type of materials used. It is also observed that the percentage of increasing the thermal conductivity for the temperature range of 20 °C to 80 °C is 23%, 33%, 23%, 27%, 24%, 29%, and 25% for samples Lo #1, Bo #2, Lo # 3, Bo # 4, Hy #5, Hy # 6, and Hy # 7, respectively. This figure also shows that at an ambient temperature of 24 °C, they have a low thermal conductivity coefficient below 0.06 W/(m K). Solid lines present the linear regression of the data in the form of

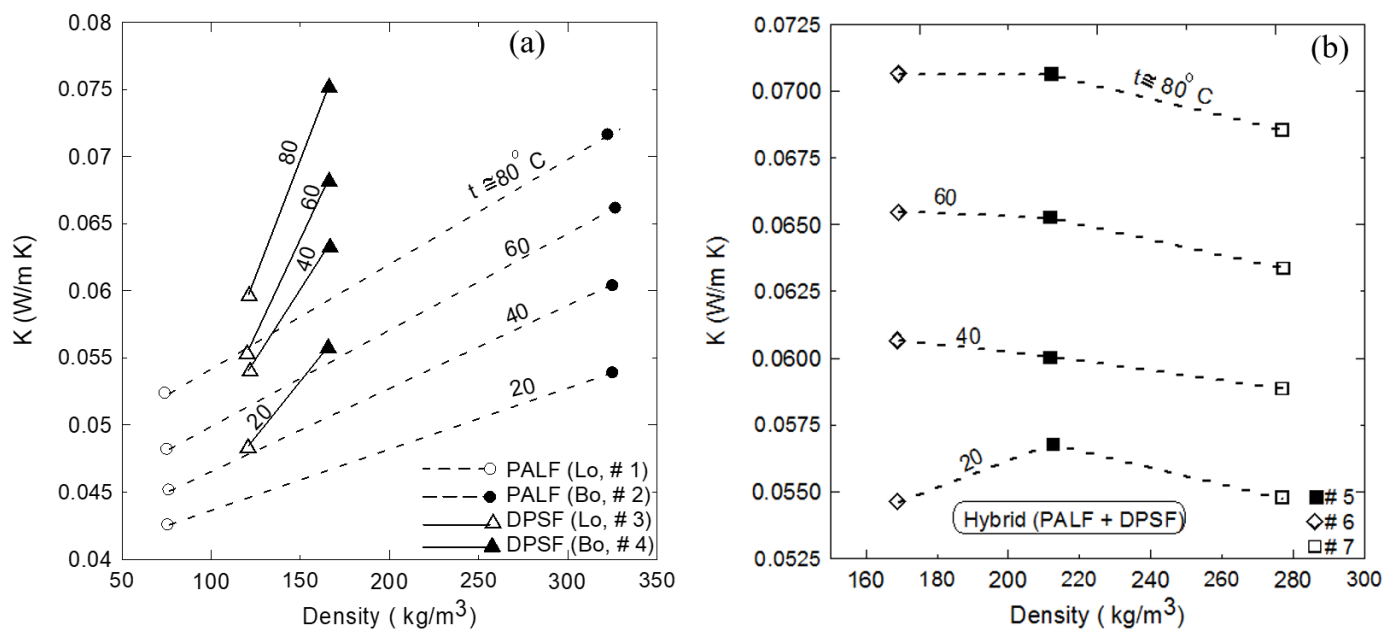
$$K = C1 + C2 t \tag{5}$$

Table 4 shows the constants C1 and C2 that appear in Equation (4), the coefficient of determination  $R^2$  of the correlation, the thermal conductivity coefficient at room temperature, and the density of each sample.

**Table 4.** Constants and  $R^2$  for correlation (1) and K at ambient temperature.

Sample Number	C1	C2	$R^2$ (%)	K at 24 °C	Density, $\text{kg/m}^3$
1 (PALF, Lo)	0.038	0.00017	99.6	0.0425	76.5
2 (PALF, Bo)	0.049	0.00028	99.9	0.0557	329
3 (DPSE, Lo)	0.046	0.00017	97.2	0.0498	121
4 (DPSE, Bo)	0.052	0.00028	99.1	0.0592	166
5(Hy)	0.051	0.00024	99.1	0.0568	212
6(Hy)	0.048	0.00028	99.6	0.0546	169
7(Hy)	0.049	0.00023	99.8	0.0547	277

Figure 13a shows the effect of density on the thermal conductivity coefficient for the same material when it is loose (with no binder) or bound at different temperatures. This figure ensures that for constant density, K increases as the temperature increases. Furthermore, adding a binder (bound composite sample) increases the density and, in turn, increases K at all temperatures. On the other hand, Figure 13b presents the variation of K with the density but for hybrid composite sample numbers 5, 6, and 7 at different temperatures. It should be noted that each curve presents three different samples, each of which may have a different polymerized binder ratio in addition to the different composition of the raw materials at each hybrid composite sample. In this case, the K profile trend looks different than that of Figure 13a due to the different compositions and the ratio of the binder of each sample; therefore, this figure summarizes the relation between K and the density at different temperatures for each hybrid composite sample. Table 5 shows a comparison between the obtained thermal conductivity and those found in the literature for similar materials.



**Figure 13.** Variation of thermal conductivity coefficients with the density of each sample at different temperatures: (a) loose and bound samples and (b) loose and hybrid samples.

**Table 5.** Range of thermal conductivity coefficients of similar materials in the literature and comparison with the ones obtained from the current study.

Polymer Fibers or Composites	Density (kg/m <sup>3</sup> )	Thermal Conductivity (w/mk)	References
PALF (Bo #2)	329	0.0541–0.0721	Current
DPSF (Bo # 4)	166	0.05918–0.075302	Current
Hy (# 5)	212	0.05679–0.070622	Current
Hy (# 6)	169	0.054595–0.07065	Current
Hy (#7)	277	0.054717–0.068542	Current
Bound sunflower seed fibers	248	0.0617–0.0801	[22]
Bound watermelon	472	0.0669–0.0982	[22]
Bound eucalyptus globulus leaves	153.0	0.0472–0.0599	[41]
Bound wheat straw fibers	130.0	0.0466–0.0569	[41]
The hybrid of eucalyptus globulus leaves and wheat straw fibers	211.0	0.0460–0.0574	[41]
Hybrid (date palm surface fibers + Apple of Sodom fibers)	114.0–233.0	0.0423–0.0529	[13]
Date palm surface fibers	176–260	0.0475–0.0697	[11]
Bagasse	70–350	0.0460–0.0550	[43]
Straw bale	50–150	0.0380–0.0670	[43]
Rice husk	154–168	0.0464–0.566	[43]
Corn cob	171–334	0.101	[44]
Jute	26.1	0.0458	[44]
Flax	32.1	0.0429	[44]
Technical hemp	30.2	0.0486	[44]
Coconut fiber	40–90	0.0480–0.0576	[45]
Kenaf	30–180	0.034–0.043	[43]

The low thermal conductivity coefficient of the bound and hybrid composites, which is below 0.07 W/(m K) at all temperature ranges up to 80 °C, promotes their use as insulation materials for buildings and other engineering applications. Figure 14 shows the sound absorption coefficient (SAC) for the bound composite sample numbers 2 and 4 and the hybrid composite ones, numbers 5, 6, and 7, for a frequency range up to 6000 Hz. In the communication range for frequencies up to 2000 Hz, it is noted that hybrid numbers 6 and 7 have SAC greater than 0.4 at a frequency of 1000 Hz and increases until 0.65 at 2000 Hz with a bell shape reaching 0.9 between 1000 and 2000 Hz. Hybrid sample number 5 has an even better SAC at the same frequency range mentioned for the other hybrid ones. On the other hand, the bound sample number 4 has the best SAC in the lower frequency range from 250 to 1000 Hz, which corresponds to SAC in general greater than 0.5. The bound sample number 2 has a lower SAC of about 0.1 up to 2000 Hz. In general, all samples exhibit high SAC at frequencies greater than 2000 Hz. The noise reduction coefficient (NRC) is determined by calculating the average value from the one-third octave values of the SAC at frequencies of 250, 500, 1000, and 2000 Hz and rounding the result to the close 0.05 following [46] and [25], as shown in Table 6. Figure 15 shows a comparison of the NRC of the samples in terms of bar charts. The SAC and the NRC indicate that in the communication range of frequency, the hybrid composite samples, and bound number 4 have good acoustic characteristics, which promote their use as sound-absorbing materials in buildings and other applications. On the other hand, at a frequency greater than 4000 Hz, all samples have good SAC, which means they have the potential to be used for

protection against noise emitted by different ultrasonic devices [47]. Moreover, it has been reported [48,49] that materials with SAC  $\geq 0.4$  can be classified as effective sound-absorbing materials and could be used for absorbing sound in engineering applications.

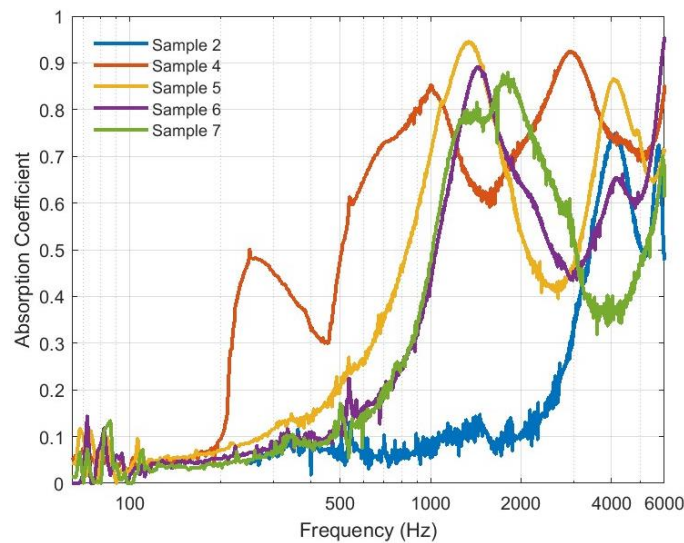


Figure 14. Sound absorption coefficients at a wide range of frequencies for the bound and hybrid samples.

Table 6. Density, sound absorption coefficients (SACs) at one-third octave values, and noise reduction coefficients (NRCs).

Sample Number	Density, kg/m <sup>3</sup>	Frequency (Hz)				NRC
		250 Hz	500 Hz	1000 Hz	2000 Hz	
Sound Absorption Coefficients (SACs)						
2	329	0.047	0.073	0.054	0.101	0.069
4	166	0.501	0.482	0.853	0.725	0.641
5	212	0.087	0.213	0.704	0.534	0.384
6	169	0.066	0.113	0.432	0.640	0.313
7	277	0.050	0.171	0.471	0.816	0.377

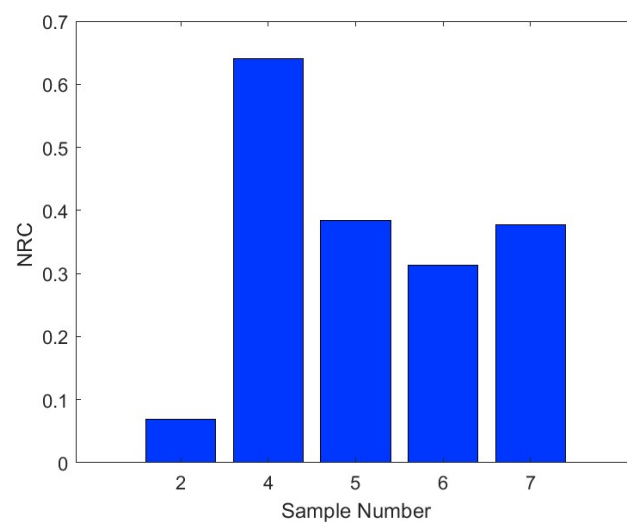


Figure 15. Noise reduction coefficients for bound and hybrid composites.

Figure 16 shows the profiles of degradation and decomposition of PALF (raw material) through the thermogravimetric analyses (TGAs) and their differential thermogravimetric analysis (DTGA) tests. This figure indicates that the PALF is stable up to about 218 °C, where the material loses its moisture content and its mass decreases by only about 10 percent (■), which corresponds to the starting of its first major degradation (■) in the DTGA profile (left). The material loses 50% of its mass (●), which is shown in the DTGA as (●) at about 315 °C. It is noted that the TGA profile has an inflection point at 372 °C (◆), where the material lost about 58% of its mass with a changing decomposition rate, where the second major degradation starts (◆), as shown on the DTGA profile. The material reaches a char at about 550 °C, where it loses about 86% of its mass (▲). This thermal characteristic and behavior of the PALF indicate that it is thermally stable up to 218 °C, which promotes its suitability for thermal insulation in buildings and other thermal insulation applications.

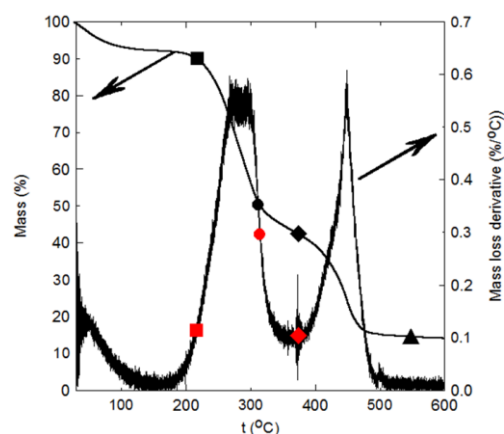


Figure 16. Thermal degradation and decomposition of PALF, see text for details.

Figure 17 presents the TGA and its DTGA for the date palm surface fibers (DPSFs). This figure indicates that the DPSF is thermally stable up to 232 °C, where the fiber loses about 8.5% of its mass (■). This point is shown as (■) in the DTGA profile, which indicates the start of the major degradation that continues up to 475 °C (◆) or (◆) on the TGA profile. The 50% degradation temperature of the fiber is approximately 364 °C (● on TGA and ● on DTGA), and the fiber reaches a char at about 1192 °C at 22% of its mass (▲). Comparison between Figures 16 and 17 confirms that DPSF is a little more thermally stable than PALF. Nevertheless, both can stand high thermal temperatures above 200 °C.

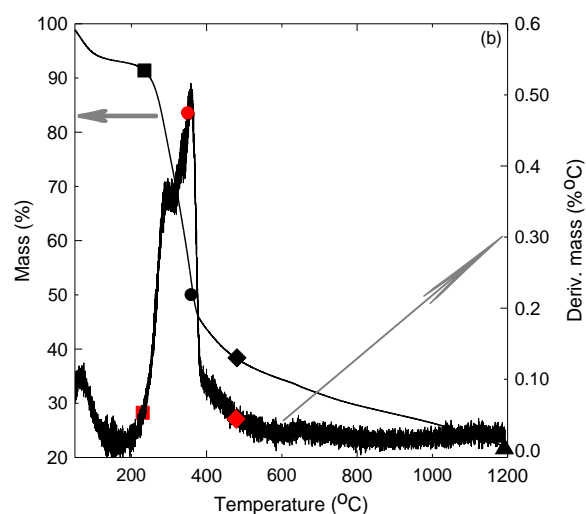
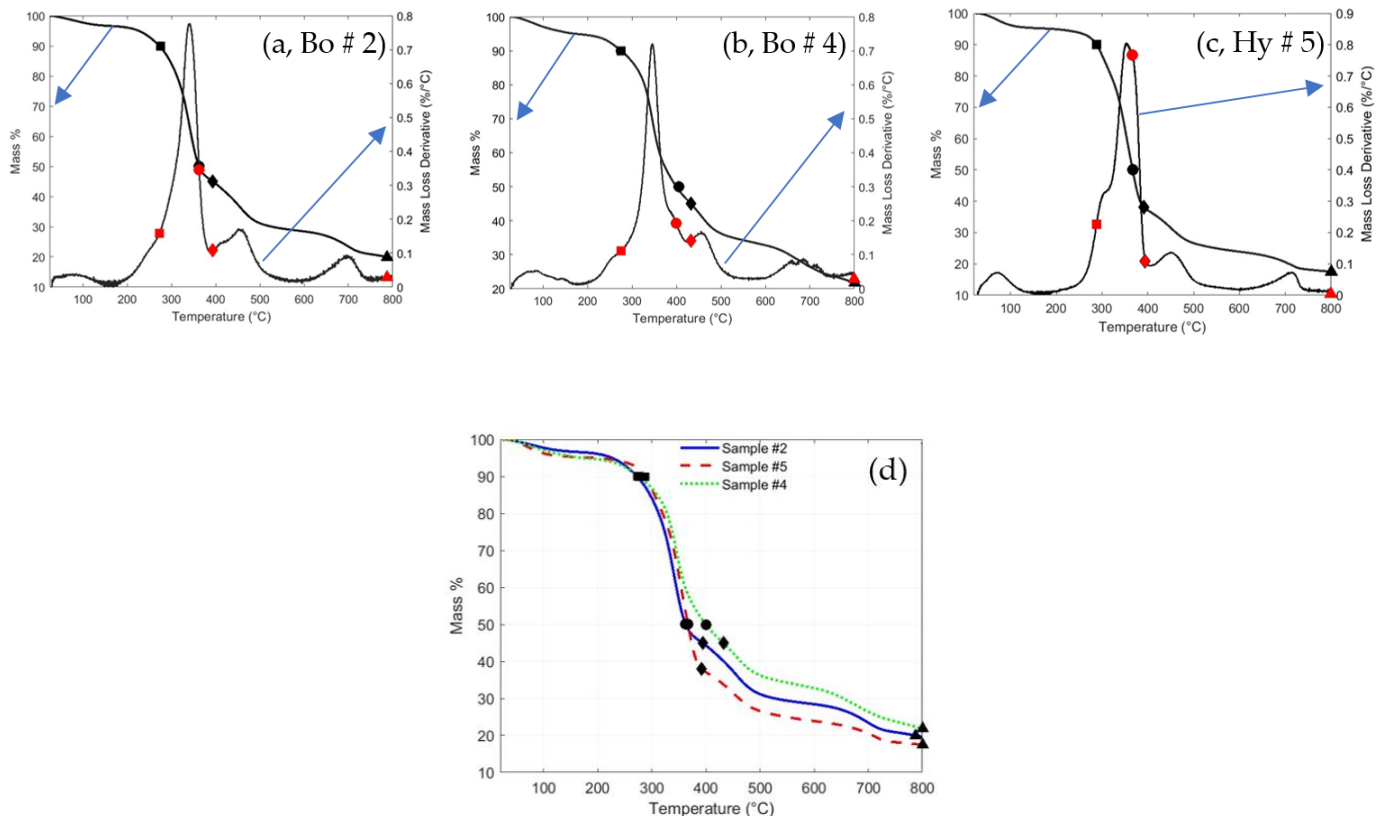


Figure 17. Thermal degradation and decomposition of DPSF, see text for details.

Figure 18a–c show the TGA and the DTGA for the bound composite sample (2), bound composite sample (4), and hybrid composite sample (5), respectively. They have similar profiles to that of Figures 16 and 17; however, each composite has its own stability, degradation, and char formation temperature, as shown in Table 7. Figure 18d shows a comparison of the TGA profiles of the bound and hybrid composites. Table 7 indicates that the bound or hybrid composites are more thermally stable than the loose fiber polymers since their thermally stable temperatures are 272.8 °C, 275.8 °C, and 287.8 °C for sample numbers 2, 4, and 5, respectively, higher than that for the loose PALF and DPSF. This observation is due to the binders.



**Figure 18.** Thermal degradation and decomposition of some composites: (a) bound of PALF sample (2), (b) bound of DPSF sample (4), (c) hybrid of PALF and DPSF sample (5), and (d) TGA profiles for the three composites, see text for details.

The bound and hybrid composites are thermally stable at higher temperatures above 200 °C, which gives them the potential to be used as safe insulation materials for buildings and other engineering applications. Figure 19a shows the moisture content profiles for the loose PALF (Lo # 1) polymer, bound (Bo # 2), bound of DPSF (Bo # 4), and hybrid composite sample numbers 5, 6, and 7 until they reach a steady state condition. This figure ensures that the PALF has a low percentage of about 4% moisture content. It is also observed that all the bound and hybrid composites have much lower moisture content (less than 2%) since most of the void porous spaces of the loose fibers are filled by the binder and hence reduce their ability to absorb more moisture. Therefore, these low moisture contents are much below the 16% that presents safe moisture content, as suggested by Bainbridge [50] for similar natural straw fibers. The moisture content for the loose DPSF polymer (Lo # 3) is presented in Figure 19b since it reaches a steady state at a longer time of about 2.5 hours. Figure 20 shows a bar chart of moisture content percentage for all samples at steady-state conditions for easier comparison.

**Table 7.** Thermally stable, T<sub>50%</sub> degradation, inflection, and char formation temperature for the bound and hybrid composites, as shown in Figure 18.

Bound Composite Sample 2 (Figure 18a)							
Thermally Stable		T <sub>50%</sub> Degradation		Inflection		Char Formation	
Mass % 90.0	Temp. (°C) 272.8	Mass % 50.0	Temp. (°C) 362.6	Mass % 45.0	Temp. (°C) 393.8	Mass % 20.0	Temp. (°C) 787.0
Hybrid composite sample 5 (Figure 18c)							
Thermally stable		T <sub>50%</sub> degradation		inflection		Char formation	
Mass % 90.0	Temp. (°C) 287.8 °C	Mass % 50.0	Temp. (°C) 366.8	Mass % 38.0	Temp. (°C) 391.7	Mass % 15.0	Temp. (°C) 800.0
Bound composite sample 4 (Figure 18b)							
Thermally stable		T <sub>50%</sub> degradation		inflection		Char formation	
Mass % 90.0	Temp. (°C) 275.8	Mass % 50.0	Temp. (°C) 400.0	Mass % 45.0	Temp. (°C) 432.5	Mass % 20.0	Temp. (°C) 800

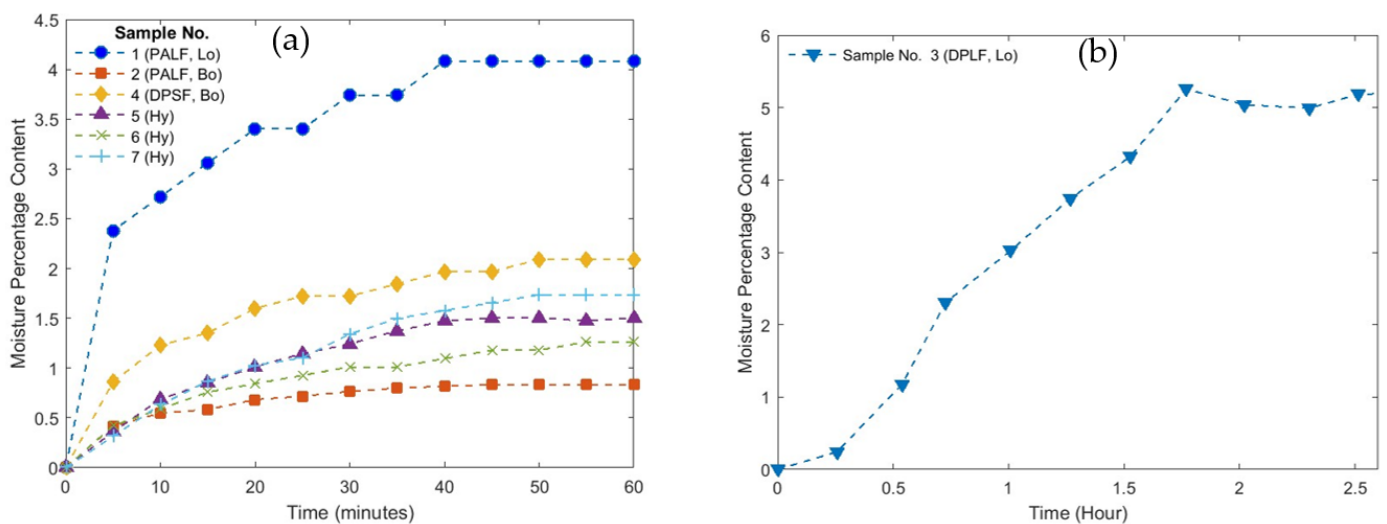


**Figure 19.** Moisture content profiles. (a) Samples 1, 2, 4, 5, 6, and 7 and (b) loose DPSF sample 3.

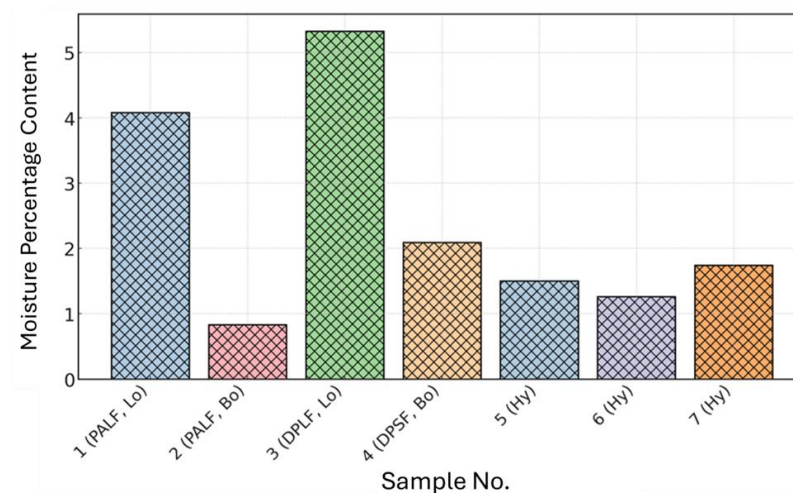


**Figure 20.** Moisture content profile for all samples at steady state conditions.

## 10. Conclusions

New hybrid polymers and composite thermal insulation and sound absorption materials were made of date palm surface fibers (DPSFs) and pineapple leaf fibers (PALFs) using wood adhesive as a binder. The result of the thermal conductivity coefficients of the samples are very optimistic and in the range of 0.042–0.06 W/(m K), 0.052–0.075 W/(m K), and 0.054–0.07 W/(m K) for the loose fiber polymers and bound and hybrid composites, respectively. The bound composite of DPSF has very good acoustic characteristics, such as a noise reduction coefficient (NRC) of 0.64 and sound absorption coefficient (SAC) greater than 0.5 for frequencies greater than 250 Hz, followed by the hybrid composites, as shown in Table 6 and Figure 14. Both raw materials of PALF and DPSF are thermally stable up to 218 °C and 232 °C, respectively. All bound and hybrid composites are thermally stable at temperatures higher than 270 °C, as shown in Table 7. Most of the bound and hybrid samples have mechanical properties such as a flexure modulus in the range of 6.47–64.16 MPa and a flexure stress range of 0.43–1.67 MPa. The loose PALF and DPSF have very low moisture contents of about 4% and 5%, respectively, and the bound composite of PALF and DPSF has a moisture content of less than 1% and about 2%, respectively. All other hybrid composites have less than 2% moisture content. These new samples of thermal insulation and sound absorption materials, either bound or hybrid, are natural, biodegradable, eco-friendly, and sustainable, which promotes them as possible replacements for synthetic and petrochemical materials in building construction and other engineering applications.

**Author Contributions:** Conceptualization, Z.A.-S., R.A., A.A. and K.A.-S.; Methodology, M.A., Z.A.-S., R.A., A.A., K.A.-S. and A.N.; Validation, Z.A.-S.; Formal Analysis, M.A., R.A. and A.N.; Investigation, Z.A.-S.; Resources, Z.A.-S. and A.N.; Data Curation, R.A., A.A. and K.A.-S.; Writing—Original Draft, K.A.-S. and A.N.; Writing—Review and Editing, M.A.; Supervision, M.A.; Project Administration, M.A. All authors have read and agreed to the published version of the manuscript.

**Funding:** The authors would like to express their appreciation for the support and funding from the Researchers Supporting Project number (RSPD2024R983), King Saud University, Riyadh, Saudi Arabia. Funding number: RSPD2024R983.

**Data Availability Statement:** The raw data supporting the conclusions of this article will be made available by the authors upon request.

**Acknowledgments:** The authors would like to thank Fahad Algubllan, Meshari Al-Howaish, Abdullah Aloraini, and Ibrahim Alqahtani for preparing some of the samples used for thermal conductivity measurements.

**Conflicts of Interest:** The authors declare that there are no conflicts of interest.

## References

1. FAO/STAT. *Crop Production, Statistics Division, Food and Agriculture Organization of United Nations*; FAO: Rome, Italy; Available online: <https://www.fao.org/food-agriculture-statistics/en/> (accessed on 20 March 2024).
2. El Morsy, M.M.S. Studies on the rachis of Egyptian date palm leaves for hardboard production. *Fibre Sci. Technol.* **1980**, *13*, 317–321. [CrossRef]
3. Barreveld, W.H. *Date Palm Products*; Bulletin No. 101; FAO Agricultural Services: Rome, Italy, 1993.
4. Khiari, R.; Mhenni, M.F.; Belgacem, M.N.; Mauret, E. Chemical composition and pulping of date palm rachis and *Posidonia oceanica*—A comparison with other wood and non-wood fibre sources. *Bioresour. Technol.* **2010**, *101*, 775–780. [CrossRef]
5. McKendry, P. Energy production from biomass (part 1): Overview of biomass. *Bioresour. Technol.* **2002**, *83*, 37–46. [CrossRef] [PubMed]
6. Nassour, A.; Majanny, A.; Nelles, M. Waste Management: Current Developments in the Arabic Countries. In Proceedings of the Tagungsband Anlässlich der Asian-European Environmental Technology and Knowledge Transfer Conference, Hefei, China, 5–6 June 2008; pp. 14–23, ISBN 978-3-00-024606-7.
7. Saidik, M.W.; El-Shaer, H.M.; Yakot, H.M. Recycling of agriculture and animal from wastes into compost using compost activator in Saudi Arabia. *J. Environ. Appl. Sci.* **2010**, *5*, 397–403.
8. Belatrache, D.; Bentouba, S.; Zioui, N.; Bourouis, M. Energy efficiency and thermal comfort of buildings in arid climates employing insulating material produced from date palm waste matter. *Energy* **2023**, *283*, 128453. [CrossRef]
9. Raza, M.; Al Abdallah, H.; Kozal, M.; Al Khaldi, A.; Ammar, T.; Abu-Jdayil, B. Development and characterization of Polystyrene-Date palm surface fibers composites for sustainable heat insulation in construction. *J. Build. Eng.* **2023**, *75*, 106988. [CrossRef]

10. Raza, M.; Al Abdallah, H.; Abdullah, A.; Abu-Jdayil, B. Date Palm Surface Fibers for Green Thermal Insulation. *Buildings* **2022**, *12*, 866. [CrossRef]
11. Ali, M.E.; Alabdulkarem, A. On thermal characteristics and microstructure of a new insulation material extracted from date palm trees surface fibers. *Constr. Build. Mater.* **2017**, *138*, 276–284. [CrossRef]
12. Ali, M.; Alabdulkarem, A.; Nuhait, A.; Al-Salem, K.; Iannace, G. Characteristics of Agro Waste Fibers as New Thermal Insulation and Sound Absorbing Materials: Hybrid of Date Palm Tree Leaves and Wheat Straw Fibers. *J. Nat. Fibers* **2022**, *19*, 6576–6594. Available online: <https://www.tandfonline.com/doi/full/10.1080/15440478.2021.1929647> (accessed on 1 June 2021). [CrossRef]
13. Alabdulkarem, A.; Ali, M.; Iannace, G.; Sadek, S.; Almuzaiqer, R. Thermal analysis, microstructure and acoustic characteristics of some hybrid natural insulating materials. *Constr. Build. Mater.* **2018**, *187*, 185–196. [CrossRef]
14. Buckle, K.A. Biotechnology Opportunities in Waste Treatment and Utilisation for The Food Industry. In *Biotechnology and The Food Industry*; Rogers, P.L., Ed.; Breach Science Publishers: New York, NY, USA, 1989; pp. 261–277.
15. Adhik, D.R.; Prasetyo, I.; Noeriman, A.; Hidayah, N.; Widayani, S. Sound Absorption Characteristics of Pineapple Leaf/Epoxy Composite. *Arch. Acoust.* **2020**, *45*, 233–240. [CrossRef]
16. Tangjuank, S. Thermal insulation and physical properties of particleboards from pineapple leaves. *Int. J. Phys. Sci.* **2011**, *6*, 4528–4532.
17. Kumfu, S.; Jintakosol, T. Thermal Insulation Produced from Pineapple Leaf and Natural Rubber Latex. *Adv. Mater. Res.* **2012**, *506*, 453–456. [CrossRef]
18. Thilagavathi, G.; Muthukumar, N.; Neela Krishnanan, S.; Senthilram, T. Development and Characterization of Pineapple Fibre Nonwovens for Thermal and Sound Insulation Applications. *J. Nat. Fibers* **2020**, *17*, 1391–1400. [CrossRef]
19. Do, N.H.; Tran, V.T.; Tran, Q.B.; Le, K.A.; Thai, Q.B.; Nguyen, P.T.; Duong, H.M.; Le, P.K. Recycling of Pineapple Leaf and Cotton Waste Fibers into Heat-insulating and Flexible Cellulose Aerogel Composites. *J. Polym. Environ.* **2021**, *29*, 1112–1121. [CrossRef]
20. Saril, K.; Isnen, Y.Z.; Utomo, A.B.; Sunardi, S. Properties of Pineapple Leaf Fibers with Paper Waste as an Absorbing-Composite to Reduce Noise. *J. Ilm. Pendidik. Fis. Al-Biruni* **2022**, *11*, 175–184. [CrossRef]
21. Suphamitmongkol, W.; Khanookon, N.; Rungruangkitkrai, N.; Boonyarit, J.; Changniam, C.; Sampoompuang, C.; Chollakup, R. Potential of Pineapple Leaf Fibers as Sound and Thermal Insulation Materials in Thailand. *Progress. Appl. Sci. Technol.* **2023**, *13*, 26–32. Available online: [https://doi.nrct.go.th/ListDoi/listDetail?Resolve\\_DOI=10.14456/past.2023.5](https://doi.nrct.go.th/ListDoi/listDetail?Resolve_DOI=10.14456/past.2023.5) (accessed on 25 March 2024).
22. Ali, M.; Al-Suhaibani, Z.; Almuzaiqer, R.; Al-Salem, K.; Nuhait, A.; Algubllan, F.; Al-Howaish, M.; Aloraini, A.; Alqahtani, I. Sunflower and Watermelon Seeds and Their Hybrids with Pineapple Leaf Fibers as New Novel Thermal Insulation and Sound-Absorbing Materials. *Polymers* **2023**, *15*, 4422. [CrossRef]
23. Namphonsane, A.; Amornsakchai, T.; Chia, C.H.; Goh, K.L.; Thanawan, S.; Wongsagonsup, R.; Smith, S.M. Development of Biodegradable Rigid Foams from Pineapple Field Waste. *Polymers* **2023**, *15*, 2895. [CrossRef]
24. Fouladi, M.H.; Nassir, M.H.; Ghassem, M.; Shamel, M.; Peng, S.Y.; Wen, S.Y.; Xin, P.Z.; Nor, M.J.M. Utilizing Malaysian natural fibers as sound absorber. In *Modeling and Measurement Methods for Acoustic Waves and for Acoustic Microdevices*; BoD—Books on Demand: Norderstedts, Germany, 2013; pp. 161–170.
25. Berardi, U.; Iannace, G. Acoustic characterization of natural fibers for sound absorption applications. *Build. Environ.* **2015**, *94*, 840–852. [CrossRef]
26. SAAF Technologies Co., Ltd., Material Safety Data Sheet Wood Adhesive 78-1040, Oct 2016, Version: R2. Available online: <https://www.gulfindustrialgroup.com/saaf/wp-content/uploads/2016/08/WOOD-ADHESIVE-78-1040-MSDS.pdf> (accessed on 20 March 2024).
27. ASTM D790-03; A Standard Test Methods for Flexural Properties of Unreinforced and Reinforced Plastics and Electrical Insulating Materials. ASTM International: West Conshohocken, PA, USA, 2003. Available online: [www.astm.org](http://www.astm.org) (accessed on 20 March 2024).
28. ASTM-C518; Standard Test Method for Steady-State Thermal Transmission Properties by Means of the Heat Flow Meter Apparatus (C 518). American Society of Testing and Materials (ASTM): West Conshohocken, PA, USA, 2010; pp. 152–166.
29. ISO 8301:1991; Thermal Insulation—Determination of Steady-State Thermal Resistance and Related Properties—Heat Flow Meter Apparatus, 1st ed.; 1991-08-01. Available online: <https://webstore.ansi.org/standards/iso/iso83011991#:~:text=ISO%208301:1991%20Thermal%20insulation%20--%20Determination%20of%20steady-state,and%20the%20calculation%20of%20its%20heat%20transfer%20properties> (accessed on 20 March 2024).
30. JIS A 1412-1:1999; Test Method for Thermal Resistance and Related Properties of Thermal Insulations—Guarded Hot Plate Apparatus, Published date 04-20-1999. Available online: [https://www.intertekinform.com/en-us/standards/jis-a-1412-1-1999-623369\\_saig\\_jsa\\_jsa\\_1436257/](https://www.intertekinform.com/en-us/standards/jis-a-1412-1-1999-623369_saig_jsa_jsa_1436257/) (accessed on 20 March 2024).
31. DIN EN 12667:2001; Thermal Performance of Building Materials and Products—Determination of Thermal Resistance by Means of Guarded Hot Plate and Heat Flow Meter Methods—Products of High and Medium Thermal Resistance; English Version of DIN EN 12667. Available online: <https://webstore.ansi.org/standards/din/dinen126672001> (accessed on 20 March 2024).
32. ISO 10534-1; Determination of Sound Absorption Coefficient and Impedance in Impedance Tubes—Part 1: Method using Standing Wave Ratio. ISO: Geneva, Switzerland, 1996.
33. ISO 10534-2; Determination of Sound Absorption Coefficient and Impedance in Impedance Tubes—Part 2: Transfer-function Method. ISO: Geneva, Switzerland, 1998.

34. Ali, M.; Almuzaiqer, R.; Al-Salem, K.; Alabdulkarem, A.; Nuhait, A. New novel thermal insulation and sound-absorbing materials from discarded facemasks of COVID-19 pandemic. *Sci. Rep.* **2021**, *11*, 23240. [[CrossRef](#)]
35. ASTM D2974-07; Standard Test Methods for Moisture, Ash, and Organic Matter of Peat and Other Organic Soils. ASTM International: West Conshohocken, PA, USA, 2007.
36. RILEM-TC. Test for the determination of modulus of rupture and limit of proportionality of thin fibre reinforced cement sections. In *RILEM Recommendations for the Testing and Use of Constructions Materials*; RILEM, Ed.; E&F Spon: London, UK, 1984; pp. 161–163, ISBN 2351580117.
37. Nguyen, D.M.; Grillet, A.-C.; Diep, T.M.H.; Bui, Q.B.; Woloszyn, M. Influence of thermo-pressing conditions on insulation materials from bamboo fibers and proteins based bone glue. *Ind. Crops Prod.* **2018**, *111*, 834–845. [[CrossRef](#)]
38. Dukhan, N.; Rayess, N.; Hadley, J. Characterization of aluminum foam–polypropylene interpenetrating phase composites: Flexural test results. *Mech. Mater.* **2010**, *42*, 134–141. [[CrossRef](#)]
39. Kline, S.J.; McClintock, F.A. Describing Uncertainties in Single-Sample Experiments. *ASME Mech. Eng.* **1953**, *75*, 3–8.
40. Moffat, R.J. Describing Uncertainties in Experimental Results. *Exp. Therm. Fluid Sci.* **1988**, *1*, 3–7. [[CrossRef](#)]
41. Ali, M.; Alabdulkarem, A.; Nuhait, A.; Al-Salem, K.; Iannace, G.; Almuzaiqer, R.; Al-Turki, A.; Al-Ajlan, F.; Al-Mosabi, Y.; Al-Sulaimi, A. Thermal and acoustic characteristics of novel thermal insulating materials made of Eucalyptus Globulus leaves and wheat straw fibers. *J. Build. Eng.* **2020**, *32*, 101452. [[CrossRef](#)]
42. Ali, M.; Alabdulkarem, A.; Nuhait, A.; Al-Salem, K.; Almuzaiqer, R.; Bayaquob, O.; Salah, H.; Alsaggaf, A.; Algafri, Z. Thermal Analyses of Loose Agave, Wheat Straw Fibers and Agave/Wheat Straw as New Hybrid Thermal Insulating Materials for Buildings. *J. Nat. Fibers* **2020**, *18*, 2173–2188. [[CrossRef](#)]
43. Asdrubali, F.; D’Alessandro, F.; Schiavoni, S. A review of unconventional sustainable building insulation materials. *Sustain. Mater. Technol.* **2015**, *4*, 1–17. [[CrossRef](#)]
44. Korjenic, A.; Petránek, V.; Zach, J.; Hroudová, J. Development and performance evaluation of natural thermal-insulation materials composed of renewable resources. *Energy Build.* **2011**, *43*, 2518–2523. [[CrossRef](#)]
45. Manohar, K.; Ramlakhan, D.; Kochhar, G.; Haldar, S. Biodegradable fibrous thermal insulation. *J. Braz. Soc. Mech. Sci. Eng.* **2006**, *28*, 45–47. [[CrossRef](#)]
46. Danihelova, A.; Nemeč, M.; Gergel, T.; Gejdos, M.; Gordanova, J.; Scensny, P. Usage of Recycled Technical Textiles as Thermal Insulation and an Acoustic Absorber. *Sustainability* **2019**, *11*, 2968. [[CrossRef](#)]
47. Pleban, D. Method of Testing of Sound Absorption Properties of Materials Induced for Ultrasonic Noise Protection. *Arch. Acoust.* **2013**, *38*, 191–195. [[CrossRef](#)]
48. Li, Y.; Ren, S. (Eds.) Building Decorative Stone. In *Woodhead Publishing Series in Civil and Structural Engineering*; Woodhead Publishing: Sawston, UK, 2011; pp. 25–53. [[CrossRef](#)]
49. Sagartzazu, X.; Hervella-Nieto, L.; Pagalday, J.M. Review in Sound Absorbing Materials. *Arch. Comput. Methods Eng.* **2008**, *15*, 311–342. [[CrossRef](#)]
50. Bainbridge, D.A. High performance low cost buildings of straw. *Agric. Ecosyst. Environ.* **1986**, *16*, 281–284. [[CrossRef](#)]

**Disclaimer/Publisher’s Note:** The statements, opinions and data contained in all publications are solely those of the individual author(s) and contributor(s) and not of MDPI and/or the editor(s). MDPI and/or the editor(s) disclaim responsibility for any injury to people or property resulting from any ideas, methods, instructions or products referred to in the content.